Evaporation residues from the fusion of ^{32}S with ^{58}Ni and ^{70}Ge observed with an energy-mass spectrograph*

D. Horn,† H. A. Enge, and A. Sperduto
Laboratory for Nuclear Science, Massachusetts Institute of Technology, Cambridge, Massachusetts 02139

A. Graue
Physics Department, University of Bergen, Bergen, Norway

(Received 27 June 1977)

Evaporation residues from the fusion reactions of 110 MeV ^{32}S with ^{58}Ni and 132 MeV ^{32}S with ^{70}Ge were observed with the aid of an energy-mass spectrograph. The residues were resolved by mass number, and the masses observed in the $^{32}S + ^{58}Ni$ reaction were $A = 84$ ($23\% \pm 5\%$), $A = 86$ ($27\% \pm 5\%$), and $A = 87$ ($50\% \pm 10\%$). The $^{32}S + ^{70}Ge$ reaction yielded $A = 94$ ($14\% \pm 1\%$), $A = 95$ ($23\% \pm 1\%$), $A = 96$ ($14\% \pm 1\%$), $A = 97$ ($24\% \pm 1\%$), $A = 98$ ($21\% \pm 1\%$), and $A = 99$ ($5\% \pm 1\%$). Angular distributions and velocity spectra were obtained for each mass, allowing partial reconstruction of the residues' kinematic history, and consequently of the particle evaporation modes leading to each residue. Average particle energies and anisotropies for each residue mass may be inferred from comparison with a Monte Carlo simulation of the evaporation process. The results are discussed and compared with calculations made with the aid of a statistical model evaporation code.

[NUCLEAR REACTIONS $^{32}S(110\ MeV_{lab}) + ^{58}Ni$ fusion, $^{32}S(132\ MeV_{lab}) + ^{70}Ge$ fusion; mass spectra, angular distributions, velocity spectra, and relative total cross sections for evaporation residues.]

I. INTRODUCTION

The formation and subsequent deexcitation of a compound nucleus are the pivotal concepts in our current understanding of a heavy-ion fusion reaction. Detection of evaporation residues, i.e., nuclei left after particle evaporation, has formerly been accomplished by the use of particle telescopes of the ΔE-E type or by time-of-flight equipment. A review of these techniques is given in a paper by Goulding and Harvey.[1] Compound-nucleus decay, following fusion, has been studied by means of charged-particle spectroscopy,[2] and identification of evaporation residues has been accomplished by measurements of characteristic in-beam γ rays and by radiochemical analysis.[3]

Much has been written about the statistical theory of the evaporation process[4-6] and about the influence of angular momentum, particularly the high-spin states produced in fusion.[7-11] Relevant experimental data have been somewhat ambiguous or do not tell the full story. Charged particle spectroscopy (protons and α particles) reveals neither the final residual nucleus nor the responsible process, which could be projectile fragmentation, preequilibrium emission, contaminant reaction, or compound-nuclear evaporation. Direct observation of the fusion product by γ spectroscopy or radiochemical analysis gives no details of the dynamics of compound-nuclear deexcitation by particle emission. Counter telescopes have proved very useful for lighter reactions[11, 12] but generally do not achieve resolution of adjacent masses for mass numbers larger than $A = 60$.

The MIT energy-mass spectrograph (EMS)[13, 14] installed at the Brookhaven double tandem Van de Graaff facility and described briefly below was designed principally to meet the need for better mass resolution in this kind of study. The first experiments performed with this instrument were studies of fusion evaporation residues of compound nuclei formed by the bombardment of two neutron-deficient targets $^{58}Ne(T_z = 1)$ and $^{70}Ge(T_z = 3)$ with a beam of $^{32}S(T_z = 0)$ ions at energies just above the Coulomb barrier. These experiments, to be described below, yielded relative production cross sections for the various evaporation residues identified by mass numbers only (A, not Z) and relative double-differential cross sections as functions of residue velocity and angle. The kinematic distributions provide information about the modes (nucleons, α particles, or a combination thereof) of evaporation and their energies, anisotropies, and sequences. Used in conjunction with the statistical model, they may also give information about the angular momentum distribution of the deexciting nuclei.

II. EXPERIMENTAL PROCEDURE

Figure 1(a) is a simplified diagram of the EMS which is described in more detail elsewhere.[13, 14] The first component after the scattering chamber is an $\vec{E} \times \vec{B}$ velocity selector (Wien filter) which

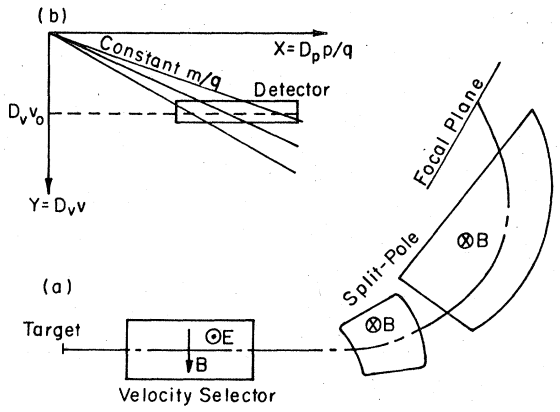

FIG. 1. (a) Simplified diagram of the EMS showing velocity selector followed by modified split-pole spectrograph. (b) Representation of focal plane showing how vertical velocity deflection and horizontal p/q deflection give rise to diagonal m/q lines in detector area.

deflects, vertically ions with a velocity differing from $v_0 = E/B$. This element is followed by a modified split-pole spectrograph deflecting the ions horizontally and analyzing them according to their momentum-charge ratio. Figure 1(b) is a simplified representation of the focal plane of the instrument indicating that horizontal displacement is linear in p/q (very nearly true) and that vertical displacement is linear in $\Delta v = v - v_0$ (less accurate). In this approximation all reaction products with a common mass-to-charge ratio fall on the focal plane along a straight line, called a mass line, through the origin. In practice, the mass lines are sharp, but slightly curved. The slope of the mass lines at a given position of the focal plane is independent of the electric field E but depends upon the ratio of the magnetic fields in the two elements. Generally, the field in the velocity selector is set at one-third the field in the split pole. The angle between the mass lines and the horizontal then varies from 17.3° at the lower end of the focal plane to 12.0° at the upper end. The range of velocities accepted by the instrument in a given exposure is about ±5%. For the experiments described here the magnetic fields were kept constant and the electric field was changed between exposures in order to cover a larger range in velocity.

In the first experiment thin ^{58}Ni foils (50–120 $\mu g/cm^2$) were bombarded with a beam of 110-MeV ^{32}S ions. The electric and magnetic fields of the spectrograph were adjusted to accept ions close in velocity v and mass-charge ratio m/q to the compound nucleus ^{90}Ru at 39 MeV.

The yields of evaporation residues in the nickel experiments were normalized to integrated current collected on a tantalum beam stop. The normalization procedure was complicated by changes of target, spectrograph solid angle, and type of beam stop. These earliest spectra were therefore interpreted in terms of *relative* abundances of each mass observed. Absolute production cross sections could, however, be obtained (Sec. III) by normalizing these relative abundances to the time-of-flight data. For all subsequent experiments, including the germanium runs, two surface-barrier detectors at 41° were used to monitor beam particles elastically scattered from the target. This ensures that the normalization is independent of target thickness, beam-charge state, type of beam stop, and number of secondary electrons emitted.

Vacuum in the EMS ranged from 10^{-5} to 3.5×10^{-6} Torr for these experiments, though better values (1.1×10^{-6} Torr) have subsequently been achieved.

Both the nickel and germanium exposures were made on Ilford 10-μm K – 2 emulsions placed in the spectrograph focal plane. Tracks from fusion evaporation residues were scanned through a microscope and observed to be on the order of 5 μm in length. The standard procedure was to count the number of tracks per mm^2 as a function of plate distance in a $\frac{1}{2}$-mm wide swath along the length of the focal plane. This produces a mass (or m/q) spectrum of particles, all having the same velocity [see Fig. 1(b)]. The scanning was done both manually at MIT and by machine at the University of Bergen in Norway. A manually scanned sample spectrum from the nickel reaction is shown in Fig. 2. The upper part of the figure results from 14-MeV sulfur particles (with $v = v_0$) in the low-energy "tail" of the beam elastically scattered from the target and from other surfaces in the same general region. The tracks of these sulfur particles are just barely distinguishable from those of the evaporation residues. The sulfur lines are quite useful since they provide a rather precise m/q calibration for a given scan along the focal plane. The lower part of Fig. 2 is an m/q spectrum of evaporation residues. The observed mass numbers are $A = 84$, 86, and 87 with charge states varying from $q = 16$ to $q = 21$. Similar m/q spectra were obtained for other velocities and angles.

For the sulfur-on-germanium reaction the situation occurs where the measurement of m/q does not always unambiguously identify a mass (e.g., $m/q = 5.000$ could be 100/20 or 95/19). The ambiguity was resolved by interpolation, making use of the periodicity of the mass peaks and the fact that they separate again at other charge states (i.e., 100/19 = 5.263 while 95/18 = 5.278).

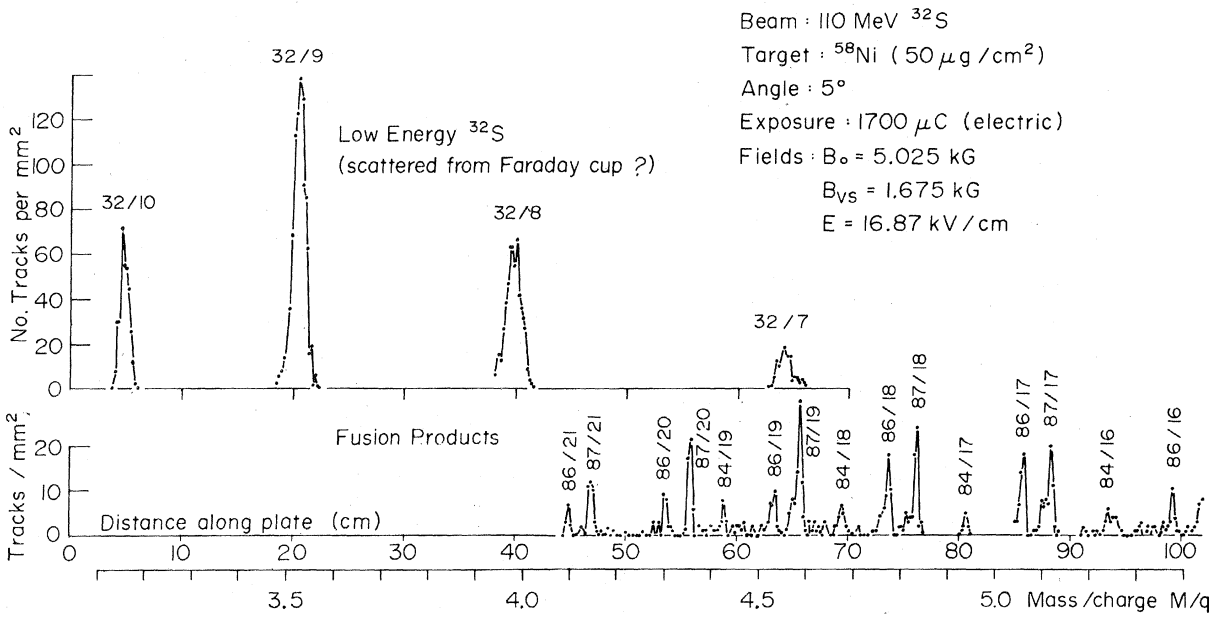

FIG. 2. Sample spectrum from ^{32}S+ ^{58}Ni reaction. Upper portion of figure is m/q spectrum of low-energy elastically scattered ^{32}S of charge states 7 to 10. Lower portion is m/q spectrum of fusion evaporation residues showing mass numbers $A=84$, 86, and 87 with charge states from 16 to 21.

III. ANALYSIS

The data were analyzed to give relative double-differential cross sections $d^2\sigma/dvd\Omega$. These were compared with the results of an evaporation kinematics code and then integrated over angle and velocity to yield total cross sections for the various mass numbers (A chains) observed.

A. Evaporation kinematics code

To relate the distributions in velocity and angle to the actual evaporations responsible for them, a Monte Carlo computer code was written for the kinematics of particle emission. The adjustable parameters for each step of the evaporation cascade leading to a given residue are particle momentum and anisotropy $\sigma_{c.m.}(0°)/\sigma_{c.m.}(90°)$. Guidance in choosing initial values for these quantities was obtained from the work of Galin *et al.*,[2] who performed light-particle spectroscopy on a compound nucleus in the same range of mass, excitation energy, and angular momentum as our ^{32}S + ^{70}Ge reaction. The parameters were then adjusted to give kinematic distributions corresponding to those observed in our reactions. An example of such a simulated kinematic distribution is shown in Fig. 3. The illustration depicts $d^2\sigma/dvd\Omega$ (lab) as a function of laboratory velocity (divided by the compound-nucleus velocity) and angle for $A=95$ from the ^{32}S + ^{70}Ge reaction. The parameters for producing this distribution will be discussed in Sec. IV.

B. Differential cross sections

The nickel data were taken at $\theta_{lab}=3°$ 5°, and the germanium data at $\theta_{lab}=3°$, 5°, and 7°. Operation

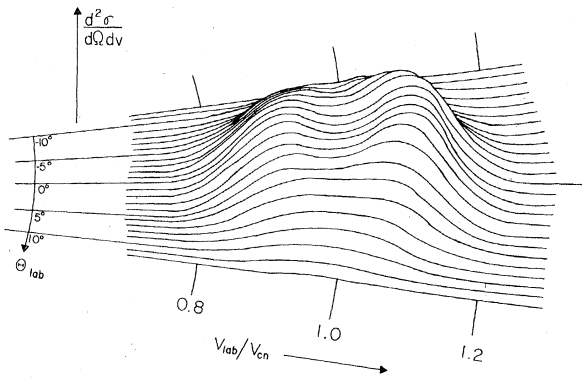

FIG. 3. Monte Carlo simulation of evaporation residue kinematic distribution for $A=95$ from the fusion of 132 MeV ^{32}S with ^{70}Ge. $d^2\sigma/d\Omega dv$ is plotted as a function of θ_{lab} and v_{lab}/v_{CN}. The curves were obtained from 9 2000 evaporation cascades, each consisting of three nucleons with average center-of-mass energies =10, 9, and 8 MeV, and one α particle with average energy =11.8 MeV. The anisotropies in the center of mass are 1.5 for the nucleons and 2.9 for the α particle. The apparent forward-backward asymmetry is a purely kinematic effect. The calculations assume $\sigma_{c.m.}(180°)=\sigma_{c.m.}(0°)$.

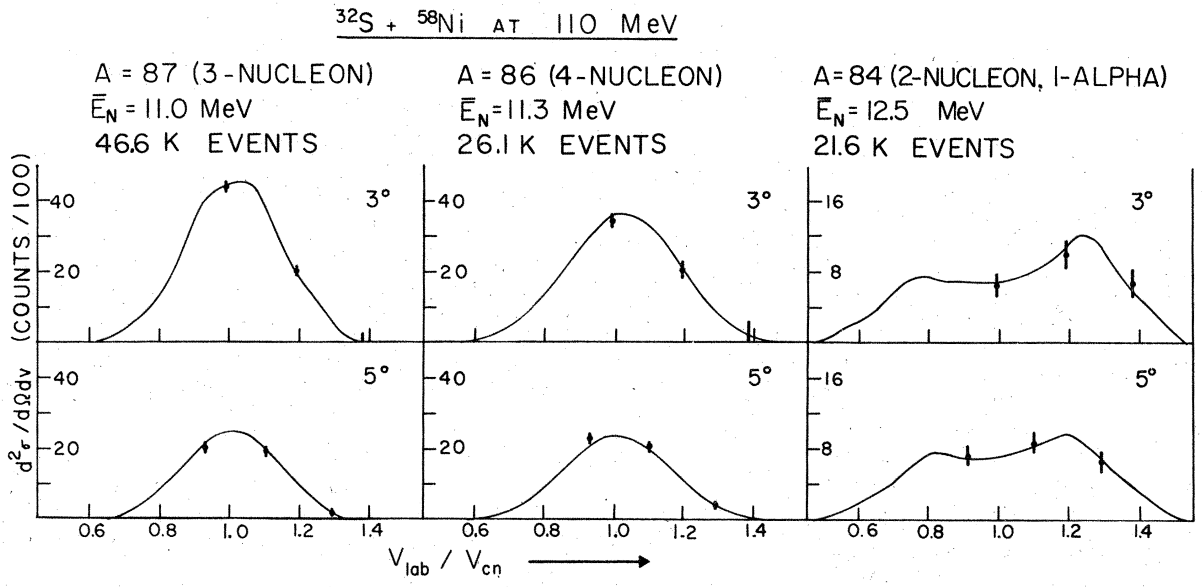

FIG. 4. Double-differential cross sections for the three A chains produced in the $^{32}S+^{58}Ni$ reaction at $\theta_{lab}=3$ and 5°. Error bars extending to $d^2\sigma/d\Omega dv=0$ give upper limits only. The curves represent Monte Carlo calculations of the residue distributions for the parameters given in the illustration. See text for anisotropies.

at $\theta_{lab}=0$ was impossible with nuclear track plate recorders because of difficulties in discriminating between evaporation residues and scattered beam particles. It has later proved to be entirely feasible to operate at $\theta_{lab}=0$ with focal-plane detectors that have better energy discrimination.

The data points for masses observed in the nickel and germanium reactions are shown in Figs. 4 and 5, respectively. Any mass not observed, e.g., $A=85$ in $^{32}S+^{58}Ni$, is believed to be of less than 5% abundance. The reference velocity v_{CN} is the calculated velocity of the compound nucleus assuming an interaction in the middle of the target. The solid curves are Monte Carlo simulations of the evaporation process, with particle types, energies, and anisotropies adjusted to fit the data points. It should be emphasized that the curves are not fits in the rigorous sense of the word; they are merely the results of several successive approximations giving a reasonably good correspondence with the data.

C. Total cross sections

Time-of-flight measurements determined the total cross section for evaporation residues of the $^{32}S+^{58}Ni$ reaction at 110 MeV to be $\sigma=310\pm50$ mb. Work performed by the Rochester group using an $E\Delta E$ counter telescope at approximately the same energy gave $\sigma=350$ mb.[15] Absolute cross sections for each mass may then be obtained from its relative intensity.

Since for every mass number the number of Monte Carlo events was chosen so as to normalize the calculation to the data, the simplest procedure for determining the relative intensity of each mass is to compare the number of Monte Carlo events. In this way, integration over velocity and angle has effectively been performed by the computer code.

Results for the three masses present in the nickel data are shown in Table I(a). Also shown are calculations made with the aid of the nuclear evaporation code ALICE,[16] with and without an option called "JANG," allowing for the removal of given amounts of angular momentum (neutron $=2\hbar$, proton $=3\hbar$, and $\alpha=10\hbar$) from the compound nucleus by the evaporated particles.

No absolute cross section was obtained for the sulfur-on-germanium reaction because the elastic scattering cross section at 41°—the monitor position—was not accurately known. Relative cross sections for the observed mass numbers are given in Table I(b) and compared with the ALICE calculations.

IV. DISCUSSION

A. $^{32}S+^{58}Ni$

The masses most strongly observed in the nickel reaction, $A=87$ and $A=86$, conform to the predictions of the ALICE calculations (see Table I) which favor three- and four-particle evaporation.

The neutron deficiency of the $^{90}_{44}Ru$ compound nucleus perturbs the usual binding energies to the point where protons are preferred for the first

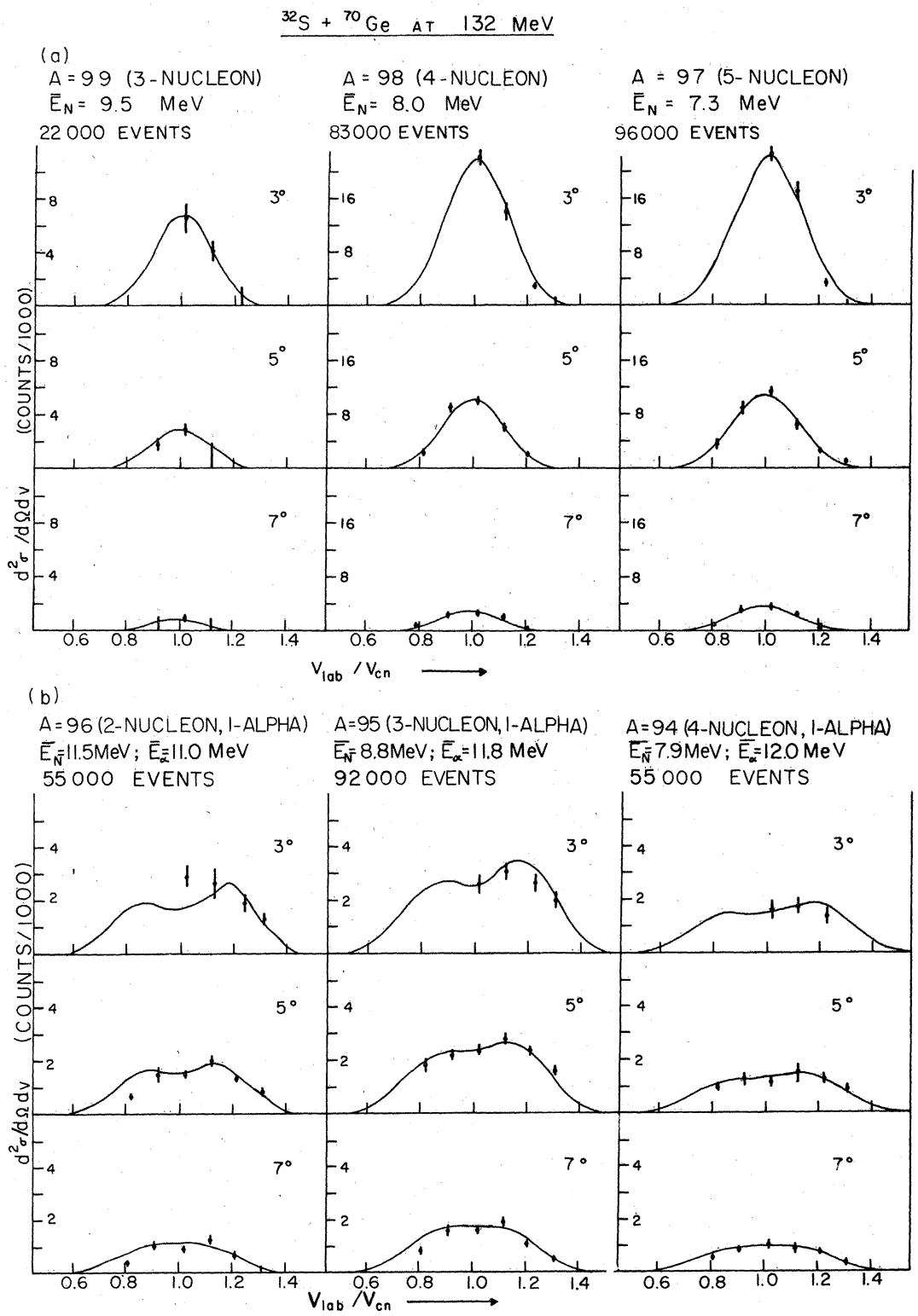

FIG. 5. (a) Double-differential cross sections for A chains produced by nucleon (only) evaporation in the $^{32}S+^{70}Ge$ reaction. Curves are calculated from the given parameters. See text for anisotropies. (b) Same as (a) for nucleon plus α evaporation.

TABLE I. Relative abundance of fusion evaporation residues.

Mass	ALICE calculation (%)	ALICE with J-loss option (%)	Experimental abundances (%)
(a) 110-MeV $^{32}S+^{58}Ni$: Compound nucleus is $^{90}_{44}Ru$, excitation=47.4 MeV			
90	•••	•••	•••
89	•••	•••	•••
88	5	2	•••
87	58	53	(50±10)
86	30	37	(27±5)
85	1	1	•••
84	5	6	(23±5)
83	1	2	•••
(b) 132.14-MeV $^{32}S+^{70}Ge$: Compound nucleus is $^{102}_{48}Cd$, excitation=72.7 MeV			
102	•••	•••	•••
101	•••	•••	•••
100	•••	•••	•••
99	10	6	(5±1)
98	21	22	(21±1)
97	12	13	(24±1)
96	11	9	(14±1)
95	21	21	(23±1)
94	15	17	(14±1)
93	3	4	trace
92	5	5	trace
91	2	3	trace

three evaporations. The fourth, going to $A=86$, could be either a proton or a neutron. The fairly compact velocity profiles of $A=87$ and $A=86$ (Fig. 3) suggest that the impulse delivered to the residue by evaporation of three or four nucleons does not drastically change its velocity from that of the compound nucleus. In mass 84, however, we see a marked deviation from simple three- or four-nucleon boiloff. Both the relative absence of $A=85$ and the binding energies calculated indicate the probable replacement of a proton by an α particle in the three-particle evaporation. A similar effect has been observed in other systems (e.g., Ref. 17 and references therein). Figure 3 offers confirmation of this hypothesis and demonstrates an advantage of the EMS: Not only is the relative abundance of each residue determined, but its angle and velocity are given as well, yielding information on the actual reaction mechanism leading to the observed residue. The velocity profile of mass 84 at 5° (lab) is much broader that that of 86 and 87. Since evaporation of an α particle over the Coulomb barrier of the compound nucleus will deliver a much larger impulse to the residue than evaporation of individual nucleons, the greater relative abundance of mass 84 at larger velocities serves as a strong indication that $A=84$ indeed results from the emission of an α particle and two nucleons. There is, in fact, a reduction in the absolute amount of $A=84$ observed at velocities close to that of the compound nucleus, which may be taken to mean that evaporation of two nucleons is generally insufficient to negate the momentum acquired by emission of one α particle. A similar reduction has been observed in a lighter system ($^{16}O+^{27}Al$) by other authors using a time-of-flight system.[12]

Mass 84 is relatively more abundant than would be predicted by the statistical theory of Weisskopf and Ewing[4] as applied in our version of the nuclear evaporation code ALICE. The model used in these calculations is, of course, quite crude. However, the discrepancy for mass 84 is large enough to call for some speculations as to its cause. A simple form of the Fermi gas level density used in these calculations is $\rho(E, J=0) \sim E^{-2} \exp 2(aE)^{1/2}$, where a is the nuclear level-density parameter, usually taken to be about $A/8$ MeV^{-1}. It is then assumed that $\rho(E, J)=(2J+1)\,\rho(E, J=0)$. This is known as the "infinite moment of inertia" or "s-wave" approximation. A more correct formulation would employ an excitation energy reduced by the amount of rotational energy in the nucleus[18]; i.e., $\rho(E) \rightarrow \rho(E-E_{\mathrm{rot}})$. When the $^{90}_{44}Ru$ compound nucleus with high spin (rms rotational energy ≈ 10 MeV) loses excitation energy through evaporation, E approaches E_{rot}. The level density of prospective daughter nuclei, which is very sensitive to the ex-

ponential term, then effectively vanishes for all possible evaporations save those which are capable of drastically reducing E_{rot}, i.e., α emission. (Competition of γ deexcitation is not discussed here. For details see Refs. 7, 9, and 10.)

Based on the above reasoning, particles and energies were proposed for the computer simulation, and the curves of Fig. 4 were obtained. For $A = 87$, three-proton evaporation with average energy $\bar{E}_N = 11.3$ MeV and average anisotropy $\sigma_{c.m.}(0°)/\sigma_{c.m.}(90°) = 1.6$ fits well. In the case of $A = 86$, four-nucleon evaporation with $\bar{E}_N = 11.0$ MeV (anisotropy = 1.6) was selected, but this was done only to fit the data points for the purposes of integration. In fact, Q-value considerations do not allow as much kinetic energy for the nucleons as would be required to reproduce the breadth of the observed kinematic distribution. This breadth may be accounted for by a small component of α or $d2p$ evaporation. Finally, two protons and one α particle give the desired curve for $A = 84$ with $\bar{E}_N = 12.5$ MeV (anisotropy = 1.4) and $\bar{E}_\alpha = 14.0$ MeV (anisotropy = 2.8).

B. $^{32}S + ^{70}Ge$

From velocity profiles of the type shown in Fig. 5(a), it is evident that masses 97, 98, and 99 have the compact distribution characteristic of individual-nucleon evaporation, while masses 94, 95, and 96 [Fig. 5(b)] have the broader distribution indicative of the evaporation of one α particle plus several nucleons. At larger laboratory angles and more extreme velocities, traces of masses 91, 92, and 93 were also observed. Their even broader and weaker kinematic distribution would logically come from two-α evaporation. The occurrence of these "groups of three" (for 0, 1, or 2 α particles) offers further corroboration of the α-substitution phenomenon discussed earlier.

For this reaction, no ambiguities were encountered of the type discussed in the previous section for $A = 86$. Masses 99 to 97 [Fig. 5(a)] fit very well with simulations of three-, four-, and five-nucleon evaporation with average nucleon energies $\bar{E}_N = 9.5$, 8.0, and 7.3 MeV (± 10%), respectively. Average anisotropies were 1.2, 1.5, and 1.5 (± 20%). For $A = 96$–94 [Fig. 5(b)] α particle plus two- to four-nucleon emission gives excellent results. $\bar{E}_N = 11.5$, 8.8, and 7.9 MeV (anisotropies of 1.2, 1.5, and 1.5) and $\bar{E}_\alpha = 11.0$, 11.8, and 12.0 MeV (anisotropies of 3.0, 2.9, and 3.0); errors correspond to those for simple nucleon emission.

Several salient features emerge from this analysis. First of all, the observed α energies of 11 to 12 MeV indicate emission below the Coulomb barrier (~14 MeV). Second, the average kinetic energy per nucleon appears to be a function of the number of emitted nucleons and independent of α emission. Figure 6 shows the nucleons' average kinetic energy as a function of number emitted. Note that additional emission of an α particle makes no significant difference. From these two points, we may surmise that these sub-Coulomb barrier α particles are emitted last and are of the type predicted by Grover and Gilat,[8] namely those required for reduction of angular momentum from points on the E-J plane for which γ-ray deexcitation is impossible or too slow.

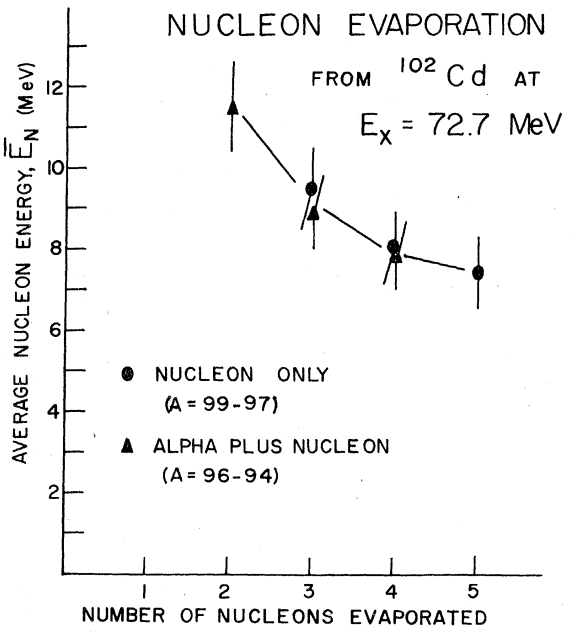

FIG. 6. Average energies of nucleons evaporated from the ^{102}Cd compound nuclear ($^{32}S + ^{70}Ge$) at 72.7 MeV excitation. Note that the average energies depend on the number of nucleons evaporated only, and not on whether an additional α particle is emitted.

Some of the velocity distributions presented in Fig. 5(b) indicate a forward-backward asymmetry of the cross section over and above the calculated "kinematic" asymmetry for residues produced by α-plus-nucleon evaporations (e.g., $A = 96$ at 5° and 7°). If this effect is real, it presumably indicates a pre-equilibrium evaporation of an α particle in the backward direction. No similar effect can be discovered in our own time-of-flight data from the $^{32}S + ^{58}Ni$ reaction, nor in the angular distributions obtained by Galin *et al.*[2] We therefore tentatively discount these observations and assign them to experimental uncertainties. We intend to make more accurate measurements, at zero degrees, when a large electronic focal-plane detector is ready.

V. CONCLUSION

Use of the EMS to investigate the compound nucleus formation-deexcitation mechanism in these sulfur-induced reactions on neutron-deficient isotopes of nickel and germanium has provided previously unobtainable data concerning the evaporation residues. In addition to the relative abundance of these residues, their kinematic coordinates are also supplied, allowing one to draw conclusions about the deexcitation mechanism.

Specifically, it was found, as had been predicted by theory, that the probability of α particle evaporation may be enhanced when the availability of energy levels in the daughter nucleus is contingent upon the removal of angular momentum by the emitted particle. Confirmation of the "replacement" phenomenon in charged-particle evaporation, whereby an α particle is emitted in place of a nucleon, was also obtained. Furthermore, a computer simulation of evaporation mechanics shows that the structure observed in the residue cross sections is a kinematic effect in agreement with (but more specific than) results of light-ion spectroscopy, making it possible to start with EMS double-differential cross sections for each residue work back through the dynamics of the evaporation cascade, assigning certain evaporation processes, particles, and energies to each residual mass.

ACKNOWLEDGMENTS

We are indebted to all members of the Heavy-Ion Group at MIT for support of various kinds. A. Luongo produced the targets and G. Young, M. Neuhausen, A. Lazzarini, and M. Salomaa all helped in obtaining the data. Discussions with W. Piel acquainted us with techniques of in-beam identification of evaporation residues from their characteristic γ rays. We also gratefully acknowledge the cooperation of the Brookhaven staff.

---

*Work supported in part by U. S. E.R.D.A. Contract No. EY-7b-C-02-3069.

†Present address: Chalk River Nuclear Laboratory, Nuclear Physics Division, Chalk River, Ontario, Canada K0J 1J0.

[1]F. S. Goulding and B. G. Harvey, Annu. Rev. Nucl. Sci. 25, 167 (1975).

[2]J. Galin, B. Gatty, D. Guerreau, C. Rousset, U. C. Schlottauer-Voos, and X. Tarrago, Phys. Rev. C 9, 1113, 1126 (1974).

[3]M. Blann and A. Ewart, Phys. Rev. 134, B783 (1964).

[4]V. F. Weisskopf and D. H. Ewing, Phys. Rev. 57, 472 (1940).

[5]T. Ericson, in *Advances in Physics*, edited by N. F. Mott (Taylor & Francis, London, 1960), Vol. 9, p. 425.

[6]J. R. Grover and J. Gilat, Phys. Rev. 157, 802 (1967).

[7]D. C. Williams and T. D. Thomas, Nucl. Phys. A92, 1 (1967).

[8]J. R. Grover and J. Gilat, Phys. Rev. 157, 815, 823 (1967).

[9]M. Blann, Phys. Rev. 157, 860 (1967).

[10]J. Gilat and J. R. Grover, Phys. Rev. C 3, 734 (1971).

[11]F. Puhlhofer, Nucl. Phys. A280, 267 (1977).

[12]B. B. Back, R. R. Betts, C. Gaarde, J. S. Larsen, E. Michelsen, and Tai Kuang-Hsi, Nucl. Phys. A285, 317 (1977).

[13]H. A. Enge, H. D. Betz, W. W. Buechner, L. Grodzins, W. H. Moore, and E. P. Kanter, Nucl. Instrum. Methods 97, 449 (1971).

[14]H. A. Enge and D. Horn, Nucl. Instrum. Methods 145 271 (1977).

[15]H. H. Gutbrod, W. G. Winn, and M. Blann, Nucl. Phys. A213, 267 (1973).

[16]M. Blann and F. Plasil, ALICE: A Nuclear Evaporation Code, U. S. Atomic Energy Commission Report No. COO-3494-10, 1973 (unpublished).

[17]J. D. Garrett, H. E. Wegner, T. M. Cormier, E. R. Cosman, and A. J. Lazzarini, Phys. Rev. C 12, 481 (1975); and T. M. Cormier, E. R. Cosman, A. J. Lazzarini, H. E. Wegner, J. D. Garrett, and F. Puhlhofer, *ibid.* 15, 654 (1977).

[18]Even this is not strictly valid; see Ref. 6.